

KA-TP-27-2001

February 8, 2020

hep-ph/01xxx

Next-to-leading order QCD corrections to $bg \rightarrow tW^-$ at the CERN Large Hadron Collider

SHOUHUA ZHU ^{*}*Institut für Theoretische Physik, Universität Karlsruhe,**D-76128 Karlsruhe, Germany*

The next-to-leading order QCD corrections to the Standard Model process of single top production, $bg \rightarrow tW^-$, for the CERN Large Hadron Collider with $\sqrt{s}=14$ TeV have been calculated. For renormalization and factorization scales $\mu = \mu_0$ ($\mu_0 = m_t + m_W$), the NLO hadronic cross section is ~ 43 pb, while ~ 26.5 pb for tree level. The NLO QCD corrections can enhance the cross section by a factor from 1.4 to 1.8 for $\frac{\mu_0}{2} < \mu < 2\mu_0$.

^{*}E-mail address: huald@particle.uni-karlsruhe.de

The top quark plays an important role for testing the standard model (SM) and searching for new physics beyond the SM, due to its large mass, the same order as the electroweak symmetry breaking scale. In order to carefully measure the top-quark electroweak interactions it is useful to consider single top production, in addition to studying the decay of the top quark in $t\bar{t}$ events. Within the context of the SM, single top production modes provide a direct measurement of the Cabibbo-Kobayashi-Maskawa matrix element V_{tb} .

At hadron colliders, single top quarks can be produced within the SM in three different channels, the s-channel W^* production [1–5], the t-channel W-exchange mode [5–12], and through tW^- production [13,14]. These three subprocesses have very different kinematics and experimental signatures, and are sensitive to different types of new physics in the top quark sector [15]. It should be noticed that the tW^- production rate is extremely small at Tevatron, but is much greater at LHC. The study shows [16] that a 5σ observation of tW^- signal is possible at very low luminosity at LHC, with 20fb^{-1} , cross section can be measured up to the accuracy of 1%.

Both the precise measurement of V_{tb} and the indirect detection of new physics require an accurate calculation of the single top quark production cross section. The QCD corrections to the s-channel W^* production [3] and the t-channel W-exchange mode [11,12] have been done. However, up to now, only part of the QCD corrections [$\mathcal{O}(1/\log m_t^2/m_b^2)$] to the cross section for $pp \rightarrow bg \rightarrow tW^-$ has been known [†] [16,17]. In this letter, the results of the complete next-to-leading-order QCD correction to tW^- production will be presented. A detailed review of the calculation will be published elsewhere [18].

The Feynman diagrams for tW^- production via the parton process $b(p_1)g(p_2) \rightarrow t(k_1)W^-(k_2)$, including the QCD corrections, are shown in Fig. 1. The Born diagrams are shown in Fig. 1(a), the NLO diagrams by virtual gluon-exchange and the gluon-radiation (gr) are shown in Fig. 1(b) and Fig. 1(c). Because the topologies of the initial-gluon (ig) diagrams are the same with the gluon-radiation processes, we don't show here the diagrams, which can be easily obtained from Fig. 1(c) by treating two gluons as initial partons. The di-

[†]In Ref. [17], the QCD corrections to the similar process of Wc production at Tevatron has been calculated.

ograms are created by use of FeynArts [19,20] and are handled with the help of FeynCalc [21]. We perform all the calculations in $d = 4 - 2\epsilon$ dimensions and adopt \overline{MS} renormalization and factorization schemes.

The total cross section for $pp \rightarrow bg \rightarrow tW^-$ at $\mathcal{O}(\alpha_s^2)$ can be written as:

$$\begin{aligned}\sigma(s) &= \sigma^0(s) + \sigma^{vir}(s) + \sigma^{gr}(s) + \sigma^{ig}(s), \\ &\equiv \sigma^{2\ body}(s) + \sigma^{gr}(s) + \sigma^{ig}(s),\end{aligned}\quad (1)$$

where

$$\begin{aligned}\sigma^{2\ body}(s) &= \int_{z_0}^1 dz \left(\frac{dL}{dz} \right)_{bg} \hat{\sigma}^{2\ body}(z^2 s, \mu_r), \\ \left(\frac{dL}{dz} \right)_{bg} &= 2z \int_{z^2}^1 \frac{dx}{x} f_{b/P}(x, \mu_f) f_{g/P}\left(\frac{z^2}{x}, \mu_f\right)\end{aligned}\quad (2)$$

with $z_0 = (m_W + m_t)/\sqrt{s}$. Here σ^0 , σ^{vir} , σ^{gr} and σ^{ig} are contributions from tree level, virtual, gluon-radiation and initial-gluon diagrams. The two-body subprocess cross section can be expressed as

$$\begin{aligned}\hat{\sigma}^{2\ body}(\hat{s}) &= \int \overline{\sum} |M_{ren}|^2 d\Phi_2 \\ &= \int \overline{\sum} |M_0|^2 d\Phi_2 + \int \overline{\sum} 2\text{Re}(M^{vir} M_0^+) d\Phi_2 \\ &\equiv \hat{\sigma}^0 + \hat{\sigma}^{vir}.\end{aligned}\quad (3)$$

Here M_0 , M_{ren} and $d\Phi_2$ are the tree level amplitude, the renormalized amplitude and the two-body phase space in d dimension. The details of the renormalization procedure and the explicit expressions of M_{ren} will be given in Ref. [18]. As usual, $\hat{\sigma}^{vir}$ contains infrared divergences after renormalization, which can only be canceled by adding contributions from σ^{gr} . The remaining collinear divergences are absorbed by the redefinition of the parton distribution functions (PDF).

The real corrections σ^{gr} and σ^{ig} have been computed using the two cut-off phase space slicing method (TCPSSM) [22]. The main idea of TCPSSM is to introduce two small constants δ_s , δ_c . The three-body phase space can then be divided into soft and hard regions according to parameter δ_s , and the hard region is further divided into collinear and non-collinear regions according to parameter δ_c . In the soft and collinear regions, approximations

can be made and analytical results can be easily obtained. In the non-collinear region, numerical results can be calculated in four dimension by standard Monte Carlo packages because it contains no divergences. The physical results should be independent on these artificial parameters δ_s and δ_c , which offers a crucial way to check our results.

We can write the σ^{gr} as

$$\sigma^{gr} = \sigma_s^{gr} + \sigma_c^{gr} + \sigma_{fin}^{gr}, \quad (4)$$

where σ_s^{gr} , σ_c^{gr} and σ_{fin}^{gr} are the contributions in the soft, collinear and non-collinear regions.

In the soft region, we can write the σ_s^{gr} as [22]

$$\begin{aligned} \sigma_s^{gr} &= \int_{z_0}^1 dz \left(\frac{dL}{dz} \right)_{bg} \hat{\sigma}_s^{gr}(z^2 s, \mu_r), \\ \hat{\sigma}_s^{gr} &= \hat{\sigma}^0 \left[\frac{\alpha_s}{2\pi} \frac{\Gamma(1-\epsilon)}{\Gamma(1-2\epsilon)} \left(\frac{4\pi\mu_r^2}{\hat{s}} \right)^\epsilon \right] \left(\frac{A_2^s}{\epsilon^2} + \frac{A_1^s}{\epsilon} + A_0^s \right). \end{aligned} \quad (5)$$

The lengthy expressions of the coefficients A_i will be given in Ref. [18]. In the collinear region, the contributions after factorization can be written as two parts [22]

$$\sigma_c^{gr} = \int_{z_0}^1 dz \hat{\sigma}^0 \left\{ \left(\frac{dL}{dz} \right)_{bg} \hat{\sigma}_c^{gr} + \left[\left(\frac{dL}{dz} \right)_{b\tilde{g}}^{gr} + \left(\frac{dL}{dz} \right)_{g\tilde{b}}^{gr} \right] \right\}, \quad (6)$$

where the definition of the luminosity is similar to that in Eq. 2. Here the \tilde{g} and \tilde{b} are

$$\tilde{g}/\tilde{b}(x, \mu_f) = \int_x^{1-\delta_s} \frac{dy}{y} f_g/f_b(x/y, \mu_f) \tilde{P}_{gg/bb}(y) \quad (7)$$

with

$$\tilde{P}_{ij}(y) = P_{ij}(y) \log \left(\delta_c \frac{1-y}{y} \frac{\hat{s}}{\mu_f^2} \right) - P'_{ij}(y), \quad (8)$$

where \hat{s} is the subprocess center-of-mass energy and

$$\begin{aligned} P_{bb}(z) &= C_F \frac{1+z^2}{1-z} \\ P'_{bb}(z) &= -C_F(1-z) \\ P_{gg}(z) &= 2N \left[\frac{z}{1-z} + \frac{1-z}{z} + z(1-z) \right] \\ P'_{gg}(z) &= 0 \end{aligned} \quad (9)$$

with $N = 3$ and $C_F = 4/3$. $\hat{\sigma}_c^{gr}$ can be written as

$$\hat{\sigma}_c^{gr} = \left[\frac{\alpha_s}{2\pi} \frac{\Gamma(1-\epsilon)}{\Gamma(1-2\epsilon)} \left(\frac{4\pi\mu_r^2}{\hat{s}} \right)^\epsilon \right] \left\{ \frac{A_1^{sc}(b \rightarrow bg)}{\epsilon} + \frac{A_1^{sc}(g \rightarrow gg)}{\epsilon} + A_0^{sc}(b \rightarrow bg) + A_0^{sc}(g \rightarrow gg) \right\}, \quad (10)$$

where

$$A_0^{sc} = A_1^{sc} \log \left(\frac{\hat{s}}{\mu_f^2} \right) \quad (11)$$

$$A_1^{sc}(b \rightarrow bg) = C_F(2 \log \delta_s + 3/2) \quad (12)$$

$$A_1^{sc}(g \rightarrow gg) = 2N \log \delta_s + (11N - 2n_f)/6 \quad (13)$$

with $n_f = 5$.

For the initial-gluon processes, the results are much simpler compared to the gluon radiation processes,

$$\sigma^{ig} = \sigma_c^{ig} + \sigma_{fin}^{ig}, \quad (14)$$

where σ_c^{ig} and σ_{fin}^{ig} are the contributions in the collinear and the non-collinear regions. After factorization, we can write σ_c^{ig} as [22]

$$\sigma_c^{ig} = \int_{z_0}^1 dz \hat{\sigma}^0 \left(\frac{dL}{dz} \right)_{g\tilde{b}}^{ig}, \quad (15)$$

where the definition of \tilde{b} in the luminosity $\left(\frac{dL}{dz} \right)_{g\tilde{b}}^{ig}$ is

$$\tilde{b}(x, \mu_f) = \int_x^1 \frac{dy}{y} f_g(x/y, \mu_f) \tilde{P}_{bg}(y). \quad (16)$$

The splitting functions in \tilde{P}_{bg} , defined in Eq. 8, contains the parts

$$\begin{aligned} P_{bg}(z) &= \frac{1}{2} [z^2 + (1-z)^2] \\ P'_{bg}(z) &= -z(1-z). \end{aligned} \quad (17)$$

Another important issue, which does not exist in gluon-radiation processes, is the procedure how to subtract the contribution of the on-shell anti-top quark decay to W^- and \bar{b} from σ^{ig} , besides subtracting double counting of $g \rightarrow b\bar{b}$ in collinear region. As in Ref. [16], in order to remove all of the \bar{t} contribution, we should subtract the term given by (in the narrow decay width limit)

$$\sigma = \sigma^{LO}(gg \rightarrow t\bar{t}) \mathcal{B}(\bar{t} \rightarrow W^- \bar{b}), \quad (18)$$

where $\sigma^{LO}(gg \rightarrow t\bar{t})$ and $\mathcal{B}(\bar{t} \rightarrow W^-\bar{b})$ are LO cross section of $gg \rightarrow t\bar{t}$ and branching ratio of the decay $\bar{t} \rightarrow W^-\bar{b}$.

Our numerical results are obtained using CTEQ5M (CTEQ5L) PDF [23] for NLO (LO) cross-section calculations. The 2-loop evolution of $\alpha_s(\mu)$ is adopted and $\alpha_s(M_Z) = 0.118$. The top-quark pole mass is taken to be $m_t = 175$ GeV; for simplicity, the bottom-quark mass has been omitted, and the renormalization and factorization scales are taken to be the same. We have compared the numerical results of the initial-gluon contribution to that in Ref. [16], and both results are in good agreement.

In Fig. 2 we show the tree level and NLO cross sections as a function of renormalization and factorization scales μ/μ_0 ($\mu_0 = m_t + m_W$). From the figure we can see that the NLO result is greater than the lowest order one. The NLO cross section is ~ 43 pb when $\mu = \mu_0$, while ~ 26.5 pb at tree level. In Fig. 3, the K factor (defined as the ratio of the NLO cross section to the LO one) is shown. For $\frac{\mu_0}{2} < \mu < 2\mu_0$, the K factor varies roughly between 1.4 and 1.8.

To summarize, the next-to-leading order QCD corrections to the Standard Model process $bg \rightarrow tW^-$ at CERN large hadron collider with $\sqrt{s} = 14$ TeV have been calculated. The NLO QCD corrections can enhance the cross section by a factor from 1.4 to 1.8 for renormalization and factorization scales $\frac{\mu_0}{2} < \mu < 2\mu_0$. We should note here that the results presented in this letter are for the process $bg \rightarrow tW^-$; they are the same for the charge conjugate process $\bar{b}g \rightarrow W^+\bar{t}$.

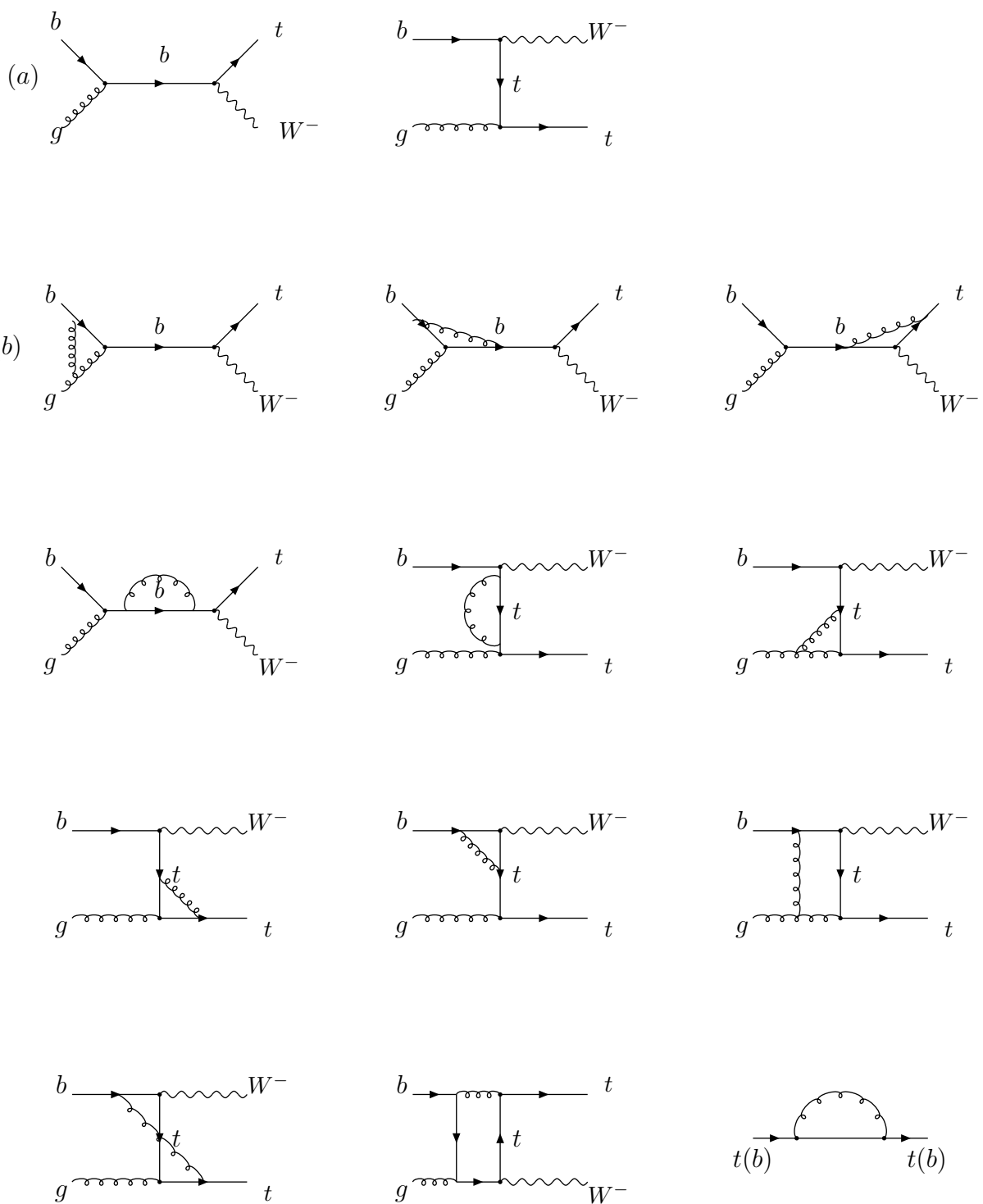
The author would like to thank Prof. W. Hollik and Prof. C.S. Li for stimulating discussions. This work was supported in part by the Alexander von Humboldt Foundation and National Nature Science Foundation of China. Parts of the calculations have been performed on the QCM cluster at the University of Karlsruhe, supported by the DFG-Forschergruppe "Quantenfeldtheorie, Computeralgebra und Monte-Carlo-Simulation".

[1] S. Cortese and R. Petronzio, Phys. Lett. B **253** (1991) 494.

- [2] T. Stelzer and S. Willenbrock, Phys. Lett. B **357**, 125 (1995) [hep-ph/9505433].
- [3] M. C. Smith and S. Willenbrock, Phys. Rev. D **54**, 6696 (1996) [hep-ph/9604223].
- [4] S. Mrenna and C. P. Yuan, Phys. Lett. B **416**, 200 (1998) [hep-ph/9703224].
- [5] A. P. Heinson, A. S. Belyaev and E. E. Boos, Phys. Rev. D **56**, 3114 (1997) [hep-ph/9612424].
- [6] S. Dawson, Nucl. Phys. B **249**, 42 (1985).
- [7] S. S. Willenbrock and D. A. Dicus, Phys. Rev. D **34**, 155 (1986).
- [8] C. P. Yuan, Phys. Rev. D **41**, 42 (1990).
- [9] R. K. Ellis and S. Parke, Phys. Rev. D **46**, 3785 (1992).
- [10] G. Bordes and B. van Eijk, Z. Phys. C **57**, 81 (1993).
- [11] G. Bordes and B. van Eijk, Nucl. Phys. B **435**, 23 (1995).
- [12] T. Stelzer, Z. Sullivan and S. Willenbrock, Phys. Rev. D **56**, 5919 (1997) [hep-ph/9705398].
- [13] G. A. Ladinsky and C. P. Yuan, Phys. Rev. D **43**, 789 (1991).
- [14] S. Moretti, Phys. Rev. D **56**, 7427 (1997) [hep-ph/9705388].
- [15] T. Tait and C. P. Yuan, hep-ph/9710372; T. Tait and C. P. Yuan, Phys. Rev. D **63**, 014018 (2001) [hep-ph/0007298].
- [16] T. M. Tait, Phys. Rev. D **61**, 034001 (2000) [hep-ph/9909352].
- [17] W. T. Giele, S. Keller and E. Laenen, Phys. Lett. B **372**, 141 (1996) [arXiv:hep-ph/9511449].
- [18] S.H. Zhu, in preparation.
- [19] J. Küblbeck, M. Böhm and A. Denner, Comput. Phys. Commun. **60**, 165 (1990).
- [20] T. Hahn, hep-ph/9905354.
- [21] R. Mertig, M. Böhm and A. Denner, Comput. Phys. Commun. **64**, 345 (1991).

[22] B. W. Harris and J. F. Owens, hep-ph/0102128; L. Reina and S. Dawson, arXiv:hep-ph/0107101; L. Reina, S. Dawson and D. Wackerlo, arXiv:hep-ph/0109066.

[23] H. L. Lai *et al.* [CTEQ Collaboration], Eur. Phys. J. C **12**, 375 (2000) [hep-ph/9903282].



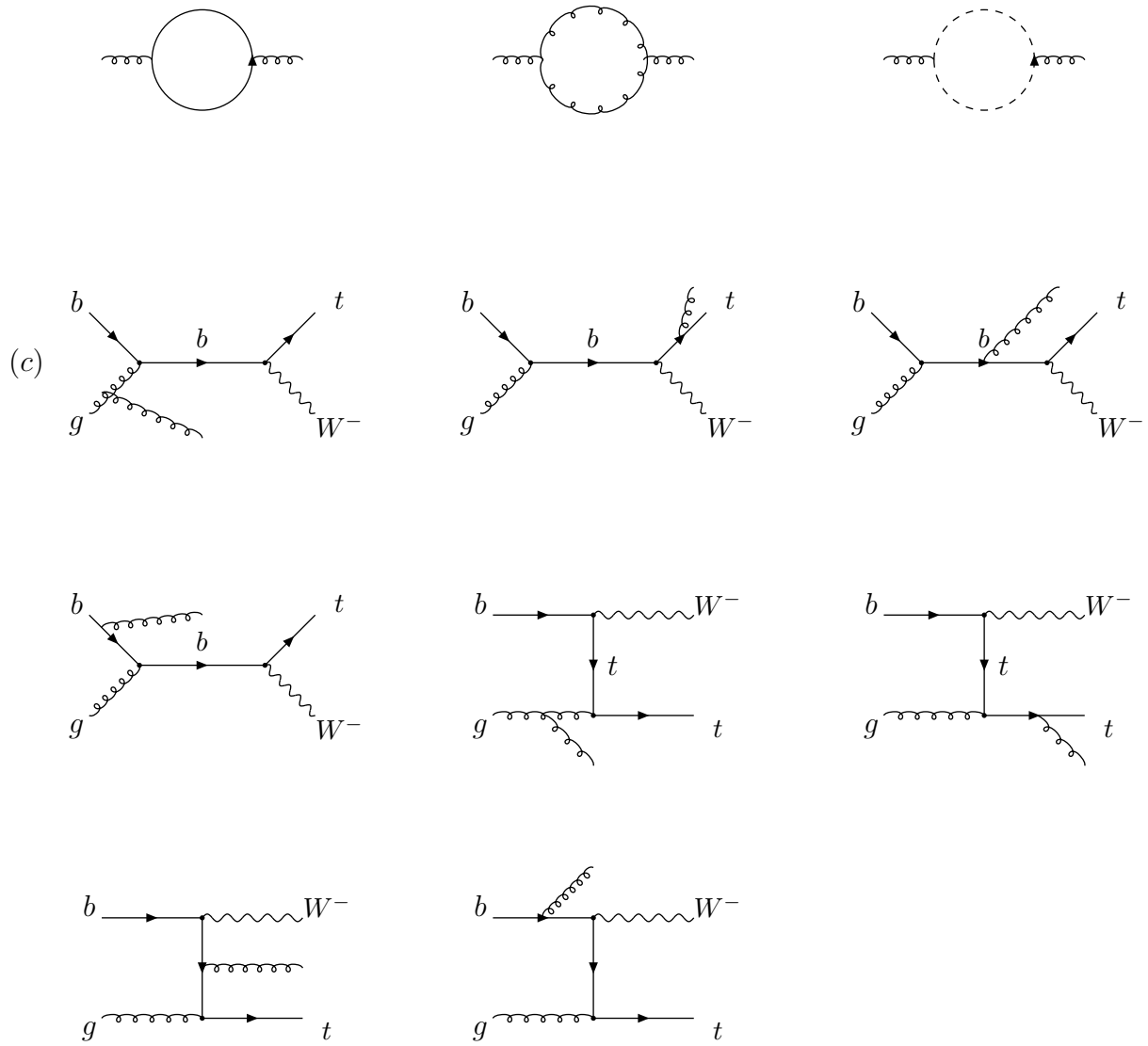


FIG. 1. Feynmann diagrams for $bg \rightarrow tW^-$: the Born level (a), the virtual gluon exchange (b) and the gluon radiation (c).

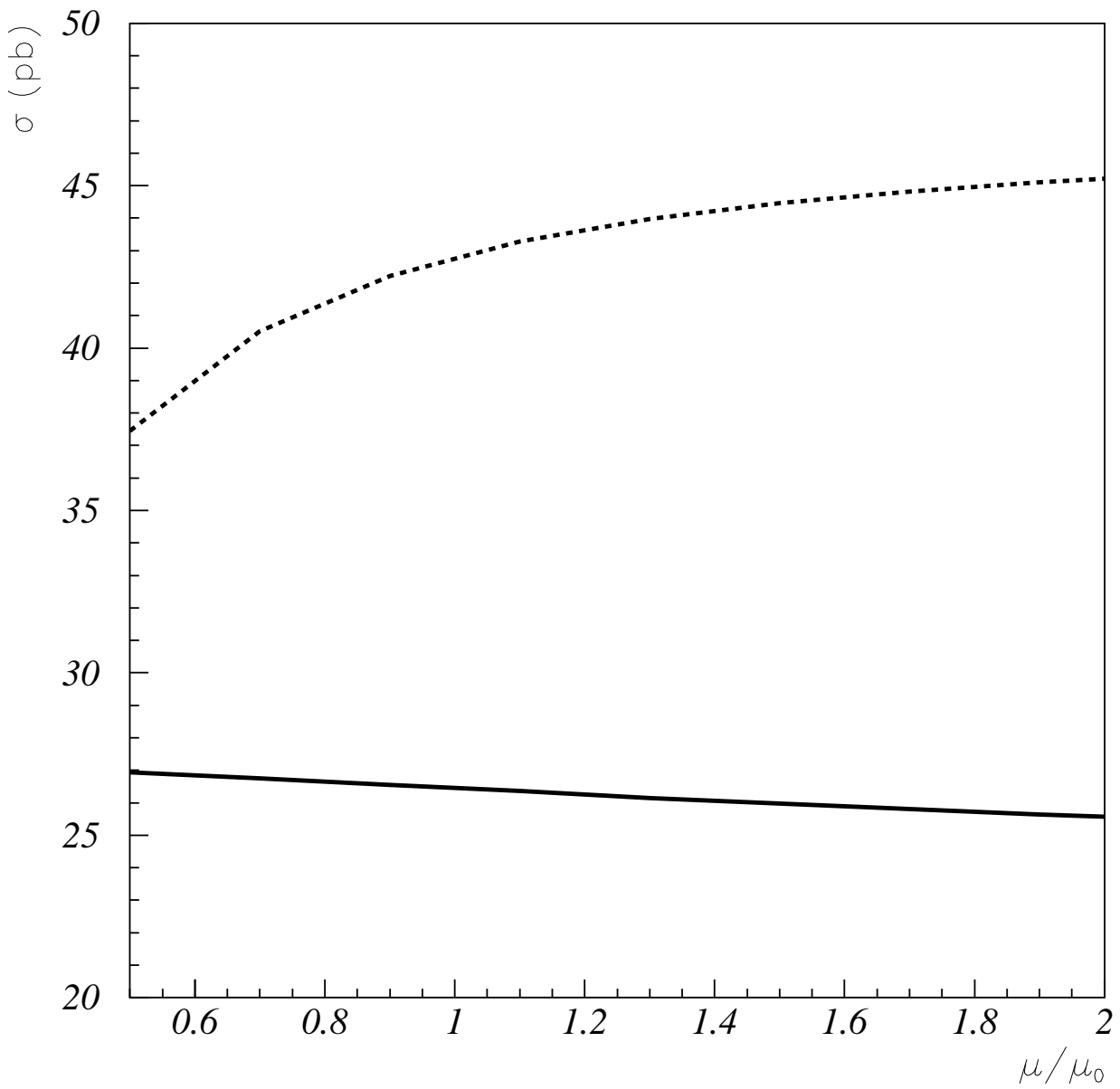


FIG. 2. Cross sections of NLO (dashed) and LO (solid) for $pp \rightarrow bg \rightarrow tW^-$ as functions of μ/μ_0 at the LHC with $\sqrt{s} = 14$ TeV, where $\mu_0 = m_t + m_W$.

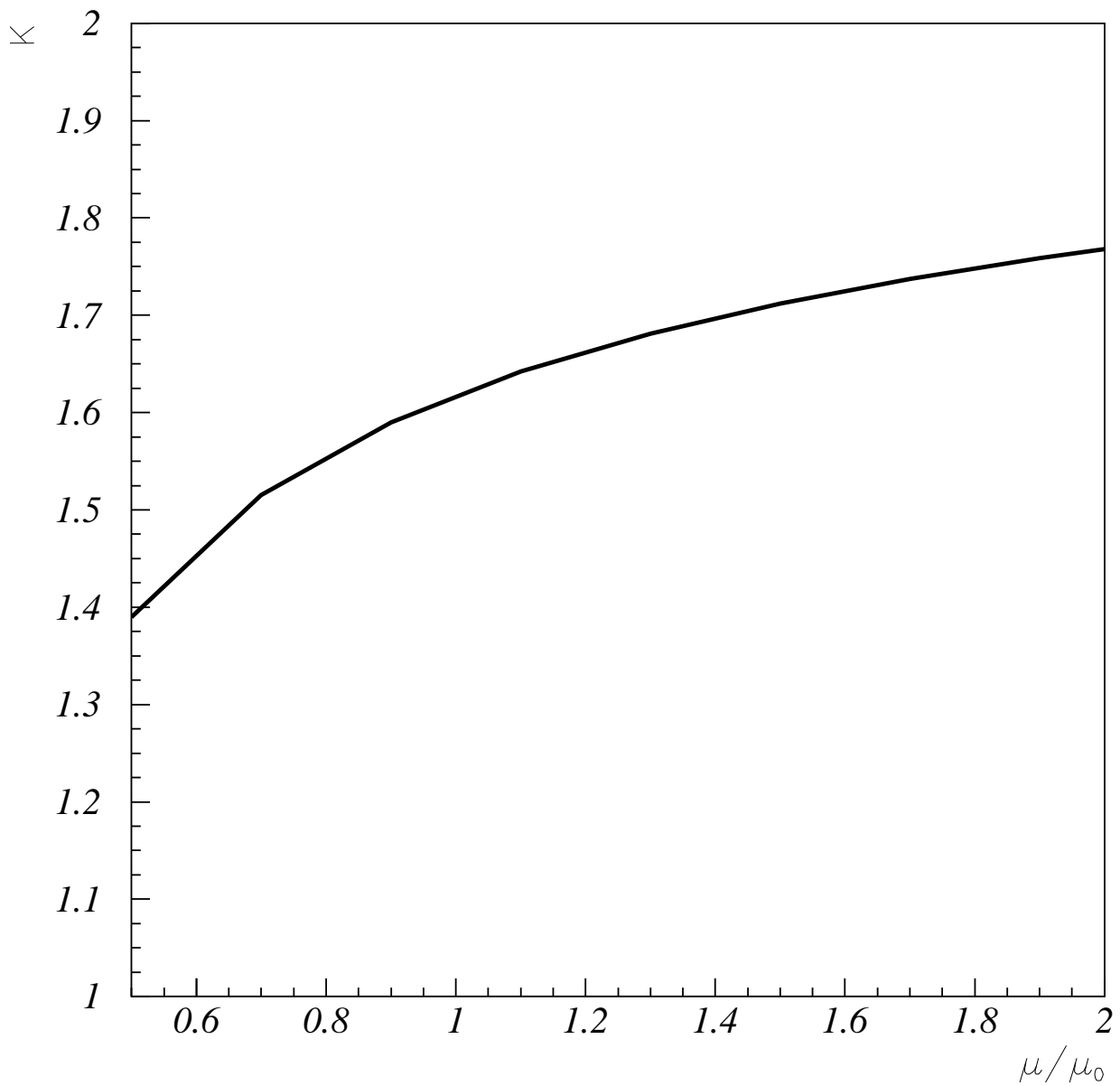


FIG. 3. K factor for $pp \rightarrow bg \rightarrow tW^-$ as functions of μ/μ_0 at the LHC.